



ELSEVIER

Contents lists available at SciVerse ScienceDirect

Superlattices and Microstructures

journal homepage: www.elsevier.com/locate/superlattices

Lead–ytterbium–telluride thin films prepared using thermal evaporation technique for thermal sensing applications

A. Hmood^{a,b,*}, A. Kadhim^{a,b}, H. Abu Hassan^a^a Nano-Optoelectronic Research and Technology Laboratory (N.O.R.), School of Physics, Universiti Sains Malaysia, 11800 USM, Penang, Malaysia^b Department of Physics, College of Science, University of Basrah, Basrah, Iraq

ARTICLE INFO

Article history:

Received 10 October 2012

Received in revised form 7 November 2012

Accepted 16 November 2012

Available online 3 December 2012

Keywords:

Pb_{1-x}Yb_xTe

Rare earth alloys and compounds

Thermoelectric generator

ABSTRACT

p-Pb_{0.925}Yb_{0.075}Te and n-Pb_{0.925}Yb_{0.075}Te powders were used in a standard synthesized solid-state microwave method to fabricate thermally evaporated thin films. The composition and microstructure of the films were studied by using X-ray diffraction and field emission scanning electron microscopy. As well as, electrical properties of the as-deposited film in terms of Seebeck coefficient, electrical conductivity, and thermoelectric (TE) power factor have been characterized at a range of 298–523 K. The micro-thermoelectric devices consisted of 20-pair and 10-pair p-Pb_{0.925}Yb_{0.075}Te:Te and n-Pb_{0.925}Yb_{0.075}Te thin films on glass substrates, respectively. The overall size of the thin-film TE generators, which comprised 20 and 10 pairs of legs connected by aluminum electrodes were 23 mm × 20 mm and 12 mm × 10 mm, respectively. The 20-pair p–n thermocouples in series generated a maximum open-circuit voltage output of 742.7 mV and a maximum output power of up to 0.657 μW at temperature difference ΔT = 162 K. In comparison, the 10-pair p–n thermocouples generated an output maximum open-circuit voltage of 467.9 mV and a maximum output power of up to 0.346 μW at ΔT = 162 K.

© 2012 Elsevier Ltd. All rights reserved.

* Corresponding author at: Nano-Optoelectronic Research and Technology Laboratory (N.O.R.), School of Physics, Universiti Sains Malaysia, 11800 USM, Penang, Malaysia. Tel.: +60 142441397; fax: +60 46579150.

E-mail address: arshad.phy73@gmail.com (A. Hmood).

1. Introduction

Improvements in thermoelectric (TE) properties of thin films over a wide temperature range have spurred interest in micro-scale TE generators [1]. These TE devices produce a few microwatts of power at relatively high voltage that used in small electric devices and systems for several applications in the microelectronics industry [2,3]. For such low-power electronics, the technology to achieve extremely low power will be necessary, and micro-scale TE devices which have so far been portable will become wearable and even implantable in the future. Micro-TE generators can be used as a power source for small electronic devices, wireless sensors and wearable electronics [4], including equipment used in military, aerospace, bio- and medical, industrial, and scientific institutions [2,5]. Advanced TE materials with potential conversion between thermal and electrical energy have been produced as a result of great scientific understanding of quantum wells and nanostructure effects on TE properties, as well as the development of modern, thin layer and nano-scale manufacturing technologies [6]. These advanced TE materials offer new opportunities for efficient and economic waste heat recovery by using highly reliable and relatively passive systems that produce no noise and vibration [7,8]. At the same time, increasing interest in producing micro-TE devices presents new opportunities in the field of micro power generation. Micro-TE converters show promise due to their high reliability, quiet operation, and environmentally friendly properties [9]. Recent developments in micro-TE devices involve the use of thin-film depositions, which are based on different growth methods such as molecular beam epitaxy (MBE) [10], metal-organic chemical-vapor deposition (MOCVD) [11], RF co-sputtering [5,12], a simple vacuum thermal evaporation [6], flash evaporation [2], and co-evaporation [4] to grow single layers and super-lattices on various substrates [2]. TE generations have primarily focused on increasing the material figure of merit (ZT), which is the standard measure of a material's TE performance. This is defined as $ZT = S^2\sigma T/\kappa$, where S is the Seebeck coefficient, σ is the electrical conductivity, κ denotes the thermal conductivity, and T is the absolute temperature. The product $S^2\sigma$ is defined as the TE power factor [13]. The power factor should be maximized and thermal conductivity should be minimized to achieve high-efficiency TE materials. In the present study, we focus on the structural characterization of thin films. Additionally, we enhance micro-fabrication methods and related electrical characterization to improve the performance and integration of micro-scale TE generators. By using a simple thermal evaporation method, we prepare $\text{Pb}_{0.925}\text{Yb}_{0.075}\text{Te}$:Te as p-type ingot and $\text{Pb}_{0.925}\text{Yb}_{0.075}\text{Te}$ as n-type ingot using a solid-state microwave synthesis for the fabrication of 20 and 10 pairs of thin-film TE micro-devices with sizes of $23\text{ mm} \times 20\text{ mm}$ and $12\text{ mm} \times 10\text{ mm}$, respectively, onto glass substrates. The intrinsic properties of each constituent thin film are investigated. The output voltage is then measured, and the maximum output power of a complete generator is estimated to be in the temperature range of 298–523 K as functions of the temperature difference between hot and cold junctions.

2. Experimental

By using a standard solid-state microwave method, an n-type $\text{Pb}_{0.925}\text{Yb}_{0.075}\text{Te}$ was synthesized as a ternary compound. Weighted 2 g amounts, according to the stoichiometric ratio $(1-x):x:1$, were prepared from three high-purity element powders (Pb , $\text{Te} \geq 99.999\%$ 100 meshes, and $\text{Yb} \geq 99.9\%$ 157 μm) as described in [14]. Polycrystalline alloys of p-type $\text{Pb}_{0.925}\text{Yb}_{0.075}\text{Te}$:Te were also prepared by using the above technique after adding excess tellurium. The thin-film TE generators were then deposited onto clean glass substrates by using thermal evaporation of 10^{-6} mbar at room temperature using baffled chimney boat manufactured by R.D. Mathis Co. (USA). The p-type ($\text{Pb}_{0.925}\text{Yb}_{0.075}\text{Te}$:Te) and n-type ($\text{Pb}_{0.925}\text{Yb}_{0.075}\text{Te}$) powders were positioned in the load cavity of the boat. When heated, the vapors of the powders followed an indirect path through a series of baffles and then exited from the vertical chimney with a height of 12 mm and a diameter of 6.3 mm. Therefore, the substrates did not encounter the bulk $\text{Pb}_{1-x}\text{Yb}_x\text{Te}$ material at any time, which essentially eliminated any chance of spitting and streaming that lead to pinholes. The distance between the boat and the substrate is 180 mm. By using an optical reflectometer (Filmatic F20, USA) measurement system, the thickness of the thin films was determined to be approximately 0.947 μm . The patterned shadow masks

fabricated 20-pair and 10-pair TE micro-devices with sizes of $23 \text{ mm} \times 20 \text{ mm}$ and $12 \text{ mm} \times 10 \text{ mm}$, respectively, for the p- and n-legs thin films and their junctions. Rectangular tracks on glass substrates for 20-pairs were $400 \mu\text{m}$ in width and 20 mm in length; for 10-pairs, the tracks had a width of $400 \mu\text{m}$ and a length of 10 mm (Fig. 1). The dimension of the p- and n-legs was 20 mm or $(10 \text{ mm}) (l) \times 400 \mu\text{m} (w) \times 0.947 \mu\text{m} (t)$, and the spacing between both legs was $150 \mu\text{m}$ (Fig. 1b). A diffusion barrier layer (Al-electrode) was also deposited between p-type and n-type thin-film TE generators at the junctions [1–7]. The fundamental physical parameters of the semiconductor lead–ytterbium–telluride thin films, such as their crystal structure, was examined by using X-ray diffraction on a PANalytical X'Pert PRO MRD PW3040 (Almelo, The Netherlands) with Cu $K\alpha$ radiation ($\lambda = 0.154060 \text{ nm}$). The morphology of the films was observed by using field emission scanning electron microscopy (FES-EM, model Leo-Supra 50 VP, Carl Zeiss, Germany). Electrical conductivity and the Seebeck coefficient were measured for the thin films within the temperature range of $298\text{--}523 \text{ K}$ between the two ends of the film. Thermal gradients with increments at both ends were also measured by using two separate thermocouples (type-K E@Sun ECS820C) that were in direct contact with the films. The output voltage

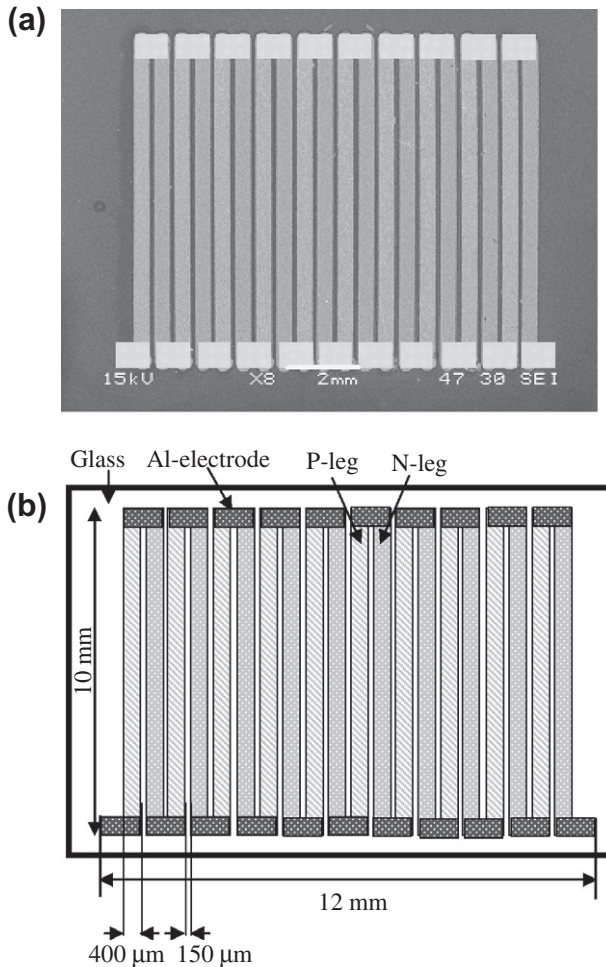


Fig. 1. (a) SEM image of 10-pair fabricated thin-film TE generator on glass substrate, and (b) schematic of thin-film TE generator.

of the thin-film TE generators was first measured while a temperature gradient $\Delta T = T_h - T_c$ was imposed between hot and cold junctions of the generators. Fig. 2 shows the schematic of the measurement for the V_{out} , output current (I_{out}), and internal resistance (R_{in}) of the thin-film thermoelectric generator. The output voltage (V_{out}), and the corresponding current (I_{out}) were measured at the Al-electrode pads connected to the TE legs. Measurement pairs of the voltage and current were acquired while load resistance R_{load} was manually adjusted. A two-wire method was used to measure the internal resistance of the thin-film TE generators. The internal resistance (R_{in}) was modified by the contact resistances that lead to $R_{in} = R_{in-ideal} + R_{contact}$ of the TE generator and was calculated as follows: $R_{in} = V_{oc}/I_{sc}$, where V_{oc} and I_{sc} represented the open-circuit voltage and the short-circuit current, respectively. The maximum output power of the thin-film TE generators was estimated from the output voltage and the overall resistance of the generators.

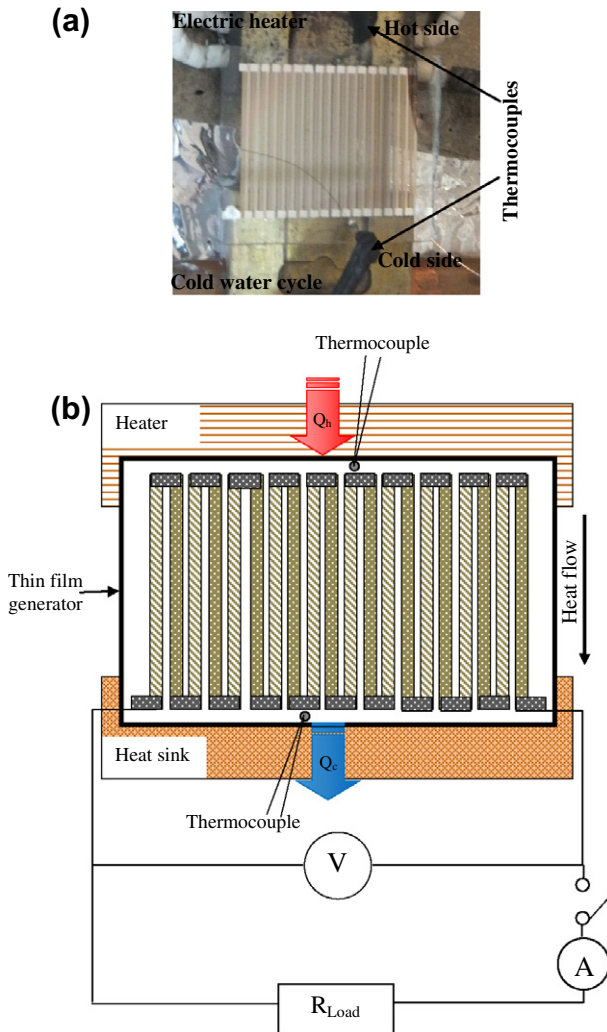


Fig. 2. (a) Photograph of 20-pair thin-film thermoelectric generator setup of the measurement of the output voltage (V_{out}) and (b) schematic of the V_{oc} of the thin-film thermoelectric generators measured as functions of the temperature difference (ΔT) between the hot and cold junctions.

3. Results and discussion

Oriented p-Pb_{0.925}Yb_{0.075}Te:Te and n-Pb_{0.925}Yb_{0.075}Te thin films with a special cubic nanostructure were synthesized by using the simple vacuum thermal evaporation method, which showed a preferential growth in the films. XRD patterns of Pb_{0.925}Yb_{0.075}Te:Te and Pb_{0.925}Yb_{0.075}Te films are shown in Fig. 3. For the Pb_{0.925}Yb_{0.075}Te:Te films, all peaks are indexed as cubic PbTe with a face-centered, rock salt (NaCl)-type structure (JCPDS 38-1435). The calculated lattice constant $a = 6.465 \text{ \AA}$ was in good agreement with previous literature data of 6.449 \AA [15], 6.453 \AA [16], and 6.464 \AA [17]. The slight increase in value was due to the change in the nature of the chemical bonding because of the substitution of Yb with Pb. Hence, being the most elongated of all, the Yb–Te distance is $\sim 3\%$ longer than the corresponding distance in YbTe (3.18 \AA), and $\sim 1.5\%$ longer than Pb–Te distance in pure PbTe (3.23 \AA) [18]. The FESEM images in Fig. 4 reveal the morphology of p-type and n-type thin films. The films are polycrystalline with preferential crystallite orientation of (200), and numerous nanocubes for Pb_{1-x}Yb_xTe material are clearly visible. It shows that Te addition tend to refine the grain growth. These changes in morphology show that with increasing Te content in the deposited film results in increase in the rate of nucleation. As a consequence, the crystallites in n-type thin film are smaller than p-type. In addition, the EDX spectra showed that the excess Te in Pb_{0.925}Yb_{0.075}Te:Te was higher than the stoichiometric ratio for the Pb_{0.925}Yb_{0.075}Te thin films without excess (Fig. 4). The actual weights (%) were experimentally equal to 41.56–53.45%, 1.69–1.60%, and 56.75–44.95% for Te, Yb, and Pb, respectively. Generally, compositions were given as n- or p-type carrier concentrations, assuming that one excess Pb atom corresponds to one free electron, and that one excess Te atom corresponds to one free hole. This result agrees well with previous report data for the material (50.1 at.% Te at 600 °C) [19]. Thus, these results correspond with the assumption on the quadruple ionization of metal vacancies in PbTe solid solutions [20].

The electrical characterizations of the as-deposited film in terms of electrical conductivity, the Seebeck coefficient, and the TE power factor were carried out at 298–523 K (Fig. 5). The electrical conductivity (σ) of both types exhibited the same increased behavior with increasing temperature, indicating

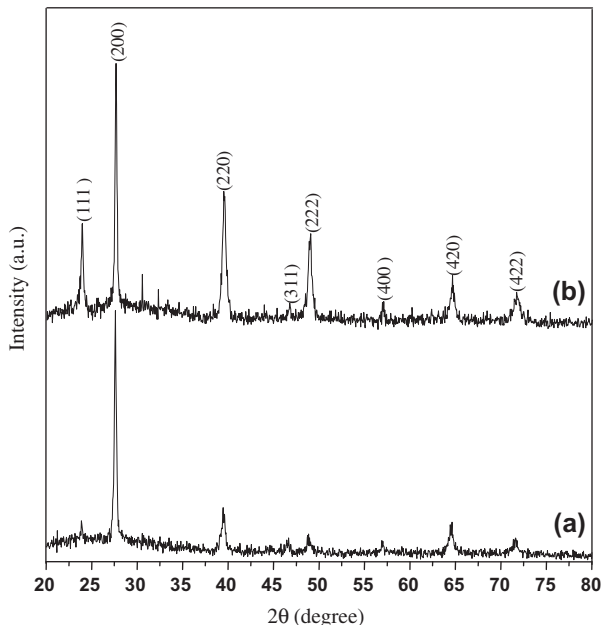


Fig. 3. XRD patterns of p-Pb_{0.925}Yb_{0.075}Te:Te (a) and n-Pb_{0.925}Yb_{0.075}Te (b) as-deposited thin films.

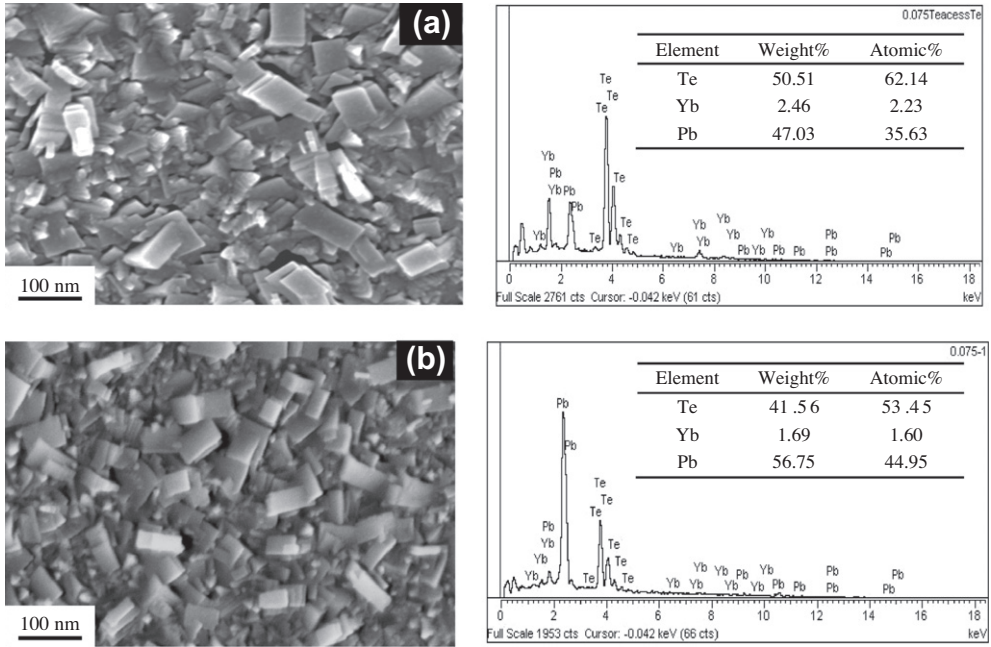


Fig. 4. FESEM images and EDX spectra of lead-ytterbium-telluride p-Pb_{0.925}Yb_{0.075}Te:Te (a) and n-Pb_{0.925}Yb_{0.075}Te (b) as-deposited thin films.

the semiconductor behavior of all alloys. The analysis of the σ behavior of both types revealed that the conduction mechanisms employ two different pathways with two different slopes, indicating the presence of two electronic transitions (Fig. 5a). The first electronic transition occurred in the low-temperature region between 3.3 K^{-1} and 2.6 K^{-1} (300–383 K), whereas the other transition occurred in the high-temperature region between 2.26 K^{-1} and 1.9 K^{-1} (443–523 K). The linearity of $\ln\sigma$ against $1/T$ for the low and high-temperature regions indicates that the $\ln\sigma$ intrinsic conduction predominates. However, in the middle-temperature region between 2.42 K^{-1} and 2.36 K^{-1} (413–423 K), the curves continuously decreased with increasing temperature, which is consistent with a degenerate semiconductor conduction caused by the density formation of states near the Fermi level [14,21].

Fig. 5b shows that the Seebeck coefficient ($S = \Delta V/\Delta T$) was determined from the slope of the thermoelectric electromotive force versus the temperature difference between the hot and cold ends of the films. The Seebeck coefficient of the p-type film (S_p) was $270.24 \mu\text{V/K}$, whereas n-type film (S_n) was $-300.24 \mu\text{V/K}$ at 523 K. Fig. 5c shows that the power factor $S^2\sigma$ for both types increased with increasing temperature range. The $S^2\sigma$ exhibited a behavior typical of semiconductors and significantly increased with increasing temperature, up to 523 K. This behavior is thus expected at high temperatures. The $S^2\sigma$ values for the n-type film were higher than those of the p-type films. The maximum value of $S_p^2\sigma_p$ was $2740.15 \mu\text{W/mK}^2$, whereas that of $S_n^2\sigma_n$ was $28459.78 \mu\text{W/mK}^2$ at 523 K. The TE generators generally depend on the Seebeck effect of heavily doped semiconductors to produce electrical energy [14–25]. In TE generation, another significant performance factor is the power factor, $S^2\sigma$ ($\text{W/K}^2 \text{ m}^{-1}$). The $S^2\sigma$ is defined as the electric power per unit area through which the heat flows per unit temperature gradient between the hot and the cold sides [26]. The fabricated micro-device of p-Pb_{0.925}Yb_{0.075}Te:Te and n-Pb_{0.925}Yb_{0.075}Te thin films are shown in Fig. 1. Seen from the top view (SEM image of Fig. 1a), the films are dense and uniform. In the experiments, the temperature difference ΔT was induced between the hot and cold junctions of the micro-generators, the output voltage was measured, and the maximum output power was estimated. Fig. 6 shows the load characteristics of the two micro-generators, namely, the current dependences of output voltage V_{out} and output power

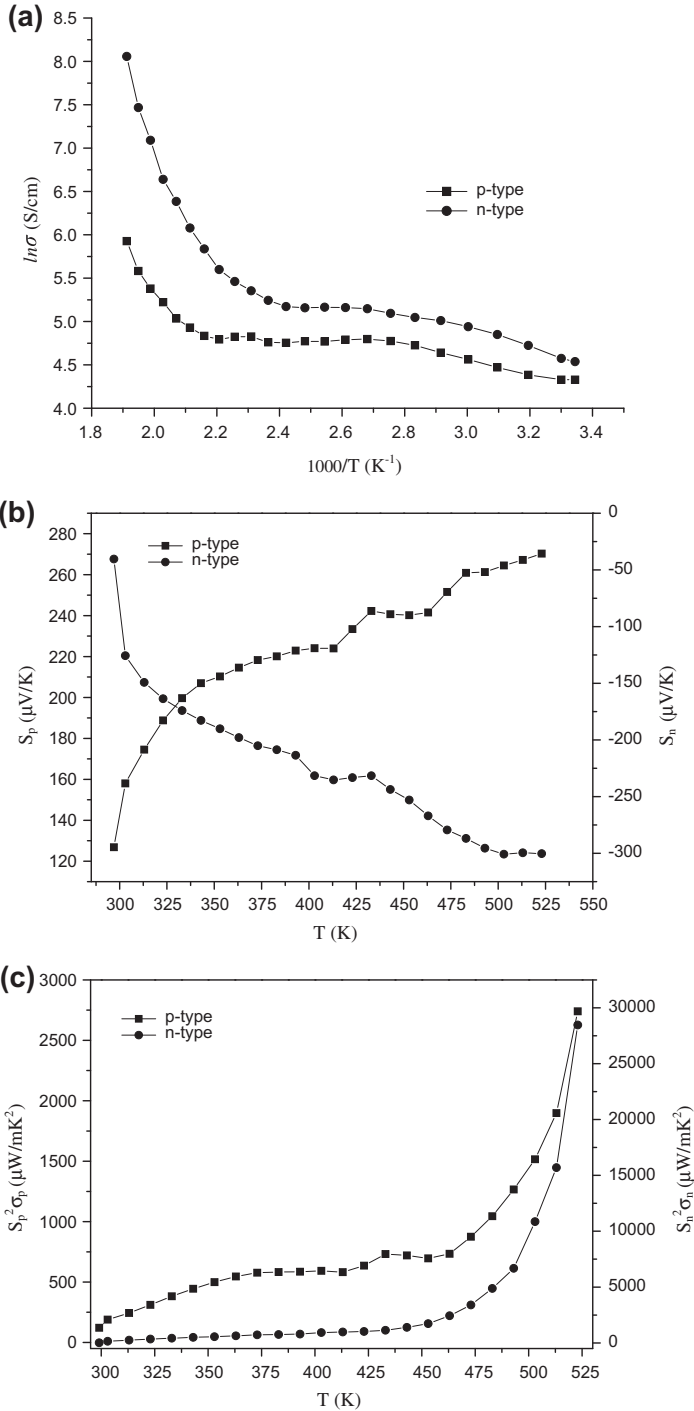


Fig. 5. Electrical transport properties of $Pb_{1-x}Yb_xTe$ thin films: (a) electrical conductivity, (b) Seebeck coefficient, and (c) power factor.

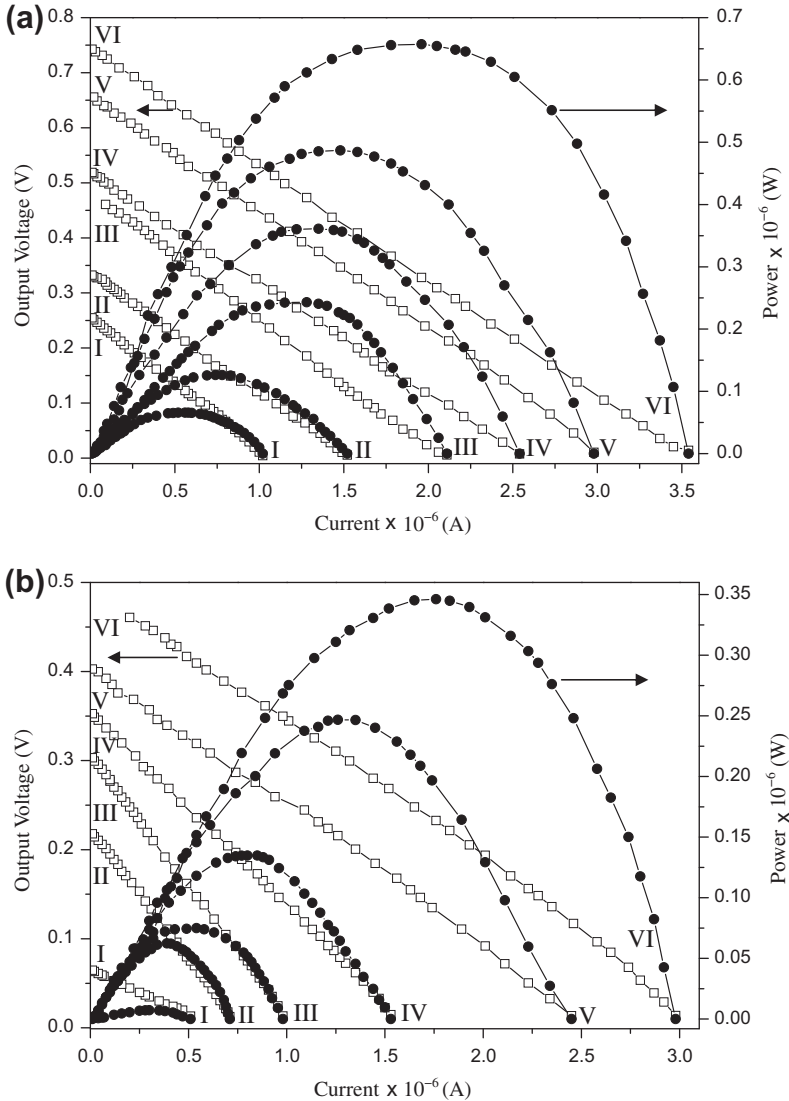


Fig. 6. Output power of the generators versus the output voltage and the output current of (a) 20-pairs $Pb_{1-x}Yb_xTe$ micro-devices with different temperature gradients ΔT at (I) $\Delta T = 75$ K, (II) $\Delta T = 92$ K, (III) $\Delta T = 112$ K, (IV) $\Delta T = 122$ K, (V) $\Delta T = 148$ K, and (VI) $\Delta T = 162$ K, and (b) 10-pairs $Pb_{1-x}Yb_xTe$ micro-devices with different temperature gradients ΔT at (I) $\Delta T = 104$ K, (II) $\Delta T = 124$ K, (III) $\Delta T = 134$ K, (IV) $\Delta T = 143$ K, (V) $\Delta T = 152$ K, and (VI) $\Delta T = 162$ K.

P_{out} as functions of the temperature difference ΔT for (a) 20-pair and (b) 10-pair microgenerators. At the temperature difference of 162 K, the output open circuit voltage (V_{oc}) and output power reach 742.7 mV and 0.657 μW , respectively, for 20-pair and 467.9 mV and 0.346 μW , respectively, for 10-pair. These results are acceptable compared with those of other materials [5,12], considering V_{oc} and maximum output power were generated under a small ΔT . The voltage or TE electromotive force (emf) produced by the Seebeck effect is defined as [9]:

$$V_{out-ideal} = n \times (S_p - S_n) \times \Delta T \tag{1}$$

where $S_{p,n}$ indicates the relative Seebeck coefficient for a material pair p–n. To maximize the generated output voltage, several thermocouples were connected electrically in a series and thermally in parallel to form a thermopile, which generated n times the output voltage of one thermocouple (if n represented the number of thermocouples in series) and a maximum output electric power P_{max} (with optimal impedance matching). This can be expressed as [27]:

$$P_{max} = \frac{(nS_{p,n}\Delta T)^2}{4R_{in}} \tag{2}$$

where R_{in} is the internal electrical resistance of the generator. The ideal internal electrical resistance $R_{in-ideal}$ is calculated from thermocouple dimensions or the number of thermocouples in series, which is defined as [28]:

$$R_{in-ideal} = n(R_p + R_n) \tag{3}$$

where R_p and R_n are the internal electrical resistance of p- and n-legs, respectively.

Assuming that the maximum output power is achieved when $R_{load} = R_{in}$, the maximum output power of micro-generators is estimated as functions of the temperature difference in the measured temperature region of $\Delta T = 162$ K [27]. The internal resistances of the micro-devices are 209.8 and 157 k Ω for the 20-pair and 10-pair, respectively. An increase in the output power P_{out} with the temperature gradient can be observed in an analysis of both plots of Fig. 6a and b. Thus, the observation results from the rise of temperature gradient ΔT which leads to an increase of output voltage V_{out} . As this output voltage increases, output current I_{out} increases (considering several values for the load resistance). Therefore, the dissipated power in the external load resistance will increase, e.g., $P_{out} = R_{load}I_{out}^2$. Fig. 6 also shows an alternative set of plots for output power P_{out} versus output current I_{out} (or versus the load resistance R_{load}). Fig. 7 shows the experimental variation in the open circuit voltage of thin-film thermoelectric generators that were measured as functions of the temperature difference between the hot and cold junctions. This result demonstrates that the devices have linear relationships with V_{oc} and ΔT . Thus, a minute amount of heat can be controlled by our device with a small ΔT . The values of ΔT applied to the micro-generators are tabulated in Table 1. This condition is attributed to the non-optimized micro-structures and to the high contact resistance caused by the non-optimized bonding process [11]. Electrical contact and thermal contact are crucial to the improvement of the device’s power generation performance; thus, related contact problems need to be minimized. From the above results, the maximum output power is instrumental to the investigation of

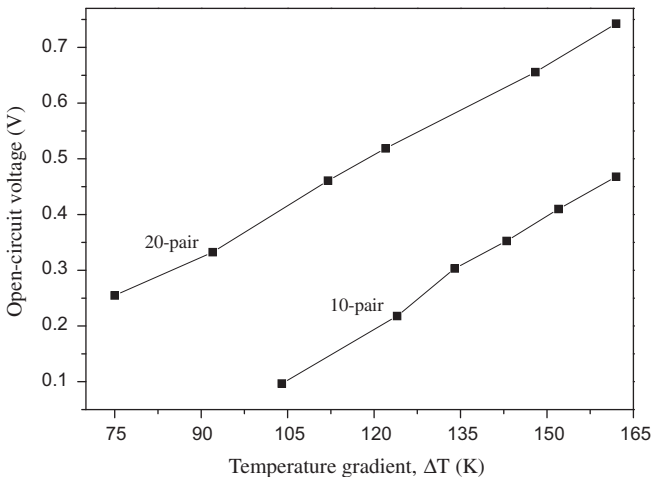


Fig. 7. Thin-film thermoelectric generator open-circuit output voltage V_{oc} various different temperature gradients ΔT .

Table 1Maximum open-circuit voltage (V_{oc}) and output power (P_{max}) at various ΔT for thin films thermoelectric generator.

Sample	ΔT (K)	104	124	134	143	152	162
10-pairs	V_{oc} (10^{-3} V)	96.71	217.8	303.2	352.6	409.9	467.9
	P_{max} (10^{-6} W)	0.007	0.062	0.075	0.135	0.247	0.346
		75	92	112	122	148	162
20-pairs	V_{oc} (10^{-3} V)	254.8	332.4	460.8	518.8	655.7	742.7
	P_{max} (10^{-6} W)	0.066	0.126	0.243	0.361	0.487	0.657

the role of the dimensions in fabricating micro-TE generators depending on the area and number of pairs of the thermocouples.

4. Conclusion

Lead-ytterbium-telluride film-based micro-generators of micro-scale design have been fabricated successfully by using a simple thermal evaporation method. The performance of the micro-generators at 298–523 K has also been measured. High output voltages of 742.7 and 467.9 mV and estimated output power of 0.657 and 0.346 μ W for 20-pair and 10-pair, respectively, have been obtained at a temperature difference of $\Delta T = 162$ K. The low power generated by each device geometry indicates that these TE configurations are not able to supply high power, but can be detected by temperature sensors due to their good voltage sensitivity. TE micro-devices exhibit scalability in output power per unit volume. The power values are low mainly due to high electrical contact resistances of the chosen device geometry.

Acknowledgments

This work was entirely supported by the Postgraduate Research Grant Scheme (PRGS) (Grant No. 1001/PFIZIK/844134) of Universiti Sains Malaysia. The authors would like to thank the Nano-Optoelectronics Research and Technology Laboratory (NOR) of the School of Physics for their assistance throughout this study.

References

- [1] M. Takashiri, T. Shirakawa, K. Miyazaki, H. Tsukamoto, *Sens. Actuators A* 138 (2007) 329–334.
- [2] G. Savelli, M. Plissonnier, J. Bablet, C. Salvi, J.M. Fournier, *MEMS/MOEMS – DTIP*, 2006, ISBN 2-916187-03-0.
- [3] Il-Ho Kim, *Mater. Lett.* 43 (2000) 221–224.
- [4] N.-H. Bae, S. Han, K.E. Lee, B. Kim, S.-T. Kim, *Curr. Appl. Phys.* 11 (2011) S40–S44.
- [5] N. Kaiwa, M. Hoshino, T. Yaginuma, R. Izaki, S. Yamaguchi, A. Yamamoto, *Thin Solid Films* 515 (2007) 4501–4504.
- [6] M. Tan, Y. Wang, Y. Deng, Z. Zhang, B. Luo, J. Yang, Y. Xu, *Sens. Actuators A* 171 (2011) 252–259.
- [7] X. Niu, J. Yu, S. Wang, *J. Power Sources* 188 (2009) 621–626.
- [8] D. Zhao, C. Tian, S. Tang, Y. Liu, L. Jiang, L. Chen, *Mater. Sci. Semicond. Process.* 13 (2010) 221–224.
- [9] L. Francioso, C. De Pascali, I. Farella, C. Martucci, P. Creti, P. Siciliano, A. Perrone, *J. Power Sources* 196 (2011) 3239–3243.
- [10] G. Zeng, J.-H. Bahk, J.E. Bowers, H. Lu, A.C. Gossard, S.L. Singer, A. Majumdar, Z. Bian, M. Zebarjadi, A. Shakouri, *Appl. Phys. Lett.* 95 (2009) 083503.
- [11] H.J. Lee, H.S. Park, S. Han, J.Y. Kim, *Thermochim. Acta* 542 (2012) 57–61.
- [12] R. Izaki, M. Hoshino, T. Yaginuma, N. Kaiwa, S. Yamaguchi, A. Yamamoto, *Microelectr. J.* 38 (2007) 667–671.
- [13] A. Hmood, A. Kadhim, H. Abu Hassan, *Superlattices Microst.* 51 (2012) 825–833.
- [14] A. Hmood, A. Kadhim, H. Abu Hassan, *J. Alloys Compd.* 520 (2012) 1–6.
- [15] B. Wan, C. Hu, B. Feng, Y. Xi, X. He, *Mater. Sci. Eng. B* 163 (2009) 57–61.
- [16] B. Wan, C. Hua, Y. Xi, J. Xu, X. He, *Solid State Sci.* 12 (2010) 123–127.
- [17] X. Chen, T.J. Zhu, X.B. Zhao, *J. Cryst. Growth* 311 (2009) 3179–3183.
- [18] I. Radisavljevic, N. Novakovic, N. Romcevic, M. Manasijevic, H.E. Mahnke, N. Ivanovic, *J. Alloys Compd.* 501 (2010) 159–163.
- [19] P. Gille, M. Muhlberg, L. Parthier, P. Rudolph, *Cryst. Res. Technol.* 19 (1984) 881–891.
- [20] G.T. Alekseeva, M.V. Vedernikov, E.A. Gurieva, L.V. Prokofeva, Y.I. Ravich, *Semiconductors* 34 (2000) 897–901.
- [21] P.M. Nikolic, D. Lukovic, S.S. Vujatovic, K.M. Paraskevopoulos, M.V. Nikolic, V. Blagojevic, et al., *J. Alloys Compd.* 466 (2008) 319–322.
- [22] Y. Pei, A.D. La Londe, S. Iwanaga, G.J. Snyder, *Energy Environ. Sci.* 4 (2011) 2085–2089.
- [23] Yu.I. Ravich, S.A. Nemov, *Semiconductors* 36 (2002) 1–20.

- [24] H.S. Dow, M.W. Oh, B.S. Kim, S.D. Park, B.K. Min, H.W. Lee, D.M. Wee1, *J. Appl. Phys.* 108 (2010) 113709.
- [25] H. Wang, Y. Pei, A.D. La Londe, G.J. Snyder, *Adv. Mater.* 23 (2011) 1366–1370.
- [26] J.P. Carmo, J. Antunes, M.F. Silva, J.F. Ribeiro, L.M. Goncalves, J.H. Correia, *Measurement* 44 (2011) 2194–2199.
- [27] L. Han, Y. Jiang, S. Li, H. Su, X. Lan, K. Qin, T. Han, H. Zhong, L. Chen, D. Yu, *J. Alloys Compd.* 509 (2011) 8970–8977.
- [28] S.-M. Choi, K.-H. Lee, C.H. Lim, W.S. Seo, *Energy Convers. Manage.* 52 (2011) 335–339.